THCz: Small molecules with antimicrobial activity that block cell wall lipid intermediates

Elisabeth Reithuber[a,1], Torbjörn Wixe[b,1], Kevin C. Ludwig[c,1], Anna Müller[c], Hanna Uvell[b], Fabian Grein[c,d], Anders E. G. Lindgren[b,e], Sandra Muschiol[a,f], Priyanka Nannapaneni[a], Anna Eriksson[b], Tanja Schneider[c,2], Staffan Normark[a,2] , Birgitta Henriques-Normark[a,f,2,3], Fredrik Almqvist[b,e,2,3] , and Peter Mellroth[a,3]

[a]Department of Microbiology, Tumor and Cell Biology, Karolinska Institutet 171 77 Stockholm, Sweden; [b]Department of Chemistry, Umeå University, Umeå 90736, Sweden; [c]Institute for Pharmaceutical Microbiology, University Hospital Bonn, University of Bonn, Bonn 53115, Germany; [d]German Center for Infection Research (DZIF), partner site Bonn-Cologne, Bonn 53115, Germany; [e]Laboratories for Chemical Biology Umeå (LCBU), Umeå University, Umeå 90736, Sweden; and [f]Clinical Microbiology, Karolinska University Hospital Solna 171 76 Stockholm, Sweden

Emerging antibiotic resistance demands identification of novel antibacterial compound classes. A bacterial whole-cell screen based on pneumococcal autolysin-mediated lysis induction was developed to identify potential bacterial cell wall synthesis inhibitors. A hit class comprising a 1-amino substituted tetrahydrocarbazole (THCz) scaffold, containing two essential amine groups, displayed bactericidal activity against a broad range of gram-positive and selected gram-negative pathogens in the low micromolar range. Mode of action studies revealed that THCz inhibit cell envelope synthesis by targeting undecaprenyl pyrophosphate–containing lipid intermediates and thus simultaneously inhibit peptidoglycan, teichoic acid, and polysaccharide capsule biosynthesis. Resistance did not readily develop in vitro, and the ease of synthesizing and modifying these small molecules, as compared to natural lipid II–binding antibiotics, makes THCz promising scaffolds for development of cell wall–targeting antimicrobials.

Streptococcus pneumoniae | antibiotic resistance | antimicrobials | cell wall biosynthesis | tetrahydrocarbazole

Since the discovery of penicillin by Alexander Fleming (1) in 1928, antibiotics have greatly improved the health quality and life expectancy of mankind. However, multidrug resistance among most microbial pathogens is reaching alarming levels, and the World Health Organization foresees a postantibiotic era where common bacterial infections may become life-threatening again due to the lack of adequate treatment regimens (2). Many of the most commonly used antibacterial drugs today, ~50% of all antibiotic prescriptions, and over 70% of intravenous applications in clinical settings, rely on inhibitors of cell wall biosynthesis (3). The essentiality of the bacterial cell wall for structural integrity and growth, and the lack of a similar structure in mammalian cells, makes the cell wall biosynthesis machinery a most attractive antibiotic target. Inhibition of cell wall synthesis can be accomplished by two main mechanisms: either by inhibition of enzyme function, for example, by beta-lactam antibiotics targeting the penicillin-binding proteins (PBPs), or by binding and blocking access to essential cell wall precursors such as the ultimate peptidoglycan building block lipid II. While a wide range of beta-lactam derivatives of different classes are continuously optimized to bypass bacterial resistance development (4), the highly conserved lipid II molecule constitutes an attractive target, as resistance development is intrinsically limited (5, 6). Lipid II is a disaccharide pentapeptide peptidoglycan subunit linked to an undecaprenyl lipid vehicle via a pyrophosphate group. It is synthesized in the cytoplasm and flipped over to the outer leaflet of the plasma membrane to provide cell wall building blocks for PBPs (7). On the outside, the ultimate peptidoglycan precursor is readily accessible for antibiotics. Presently, lipid II–binding antibiotics of at least five chemical classes are known, comprising glycopeptides (e.g., vancomycin) (8), lantibiotics (e.g., nisin), defensins (e.g.,

plectasin), lipopeptides (e.g., empedopeptin), and depsipeptides (e.g., teixobactin) (9, 10). More recently, the last-resort antibiotic daptomycin was further shown to target undecaprenyl-containing lipid intermediates (11). In common for these agents is that binding to lipid II sequesters the molecule and makes it unavailable for peptidoglycan biosynthesis. However, antibiotic activities can vary substantially depending on the binding site on the lipid II molecule (6). Vancomycin, for example, binds to the terminal D-alanyl-D-alanine residue of the lipid II stem peptide, a part of the molecule that is altered in resistant strains. In contrast, resistance development to compounds that recognize the pyrophosphate moiety as minimal binding motif, which is present in several cell wall intermediates from different pathways (i.e., peptidoglycan, wall teichoic acid, and capsule biosynthesis), is strongly hampered. This structural feature is highly conserved among bacteria, and direct target modifications have not been observed (7).

The vast majority of lipid II–binding antibiotics described so far mainly act on gram-positive bacteria, since the outer membrane of gram-negative bacteria restricts target access mainly due to the large size of these compounds. Notably, no small-molecule inhibitor (< 500 Da) targeting lipid II has been identified so far.

Here, we developed a bacterial whole-cell screening platform aimed to identify small molecules with cell wall synthesis

Significance

Considering the alarming emergence of resistance to most antibiotics and the need for new antibiotics, the finding here of a small-molecule class, THCz, that displayed bactericidal activity against gram-positive and selected gram-negative bacteria, is of the greatest importance. We found that THCz target the cell envelope synthesis and can easily be synthesized and modified, and resistance did not readily develop in vitro. Thus, THCz are promising scaffolds for development of bacterial cell wall inhibitors.

inhibiting activity. The screen used the induction of autolysin-mediated lysis as a phenotypic readout for cell wall inhibition. It is well established that cell wall targeting agents, in addition to stalling cell wall synthesis, can also trigger activation of endogenous bacterial autolysins that facilitate cell wall degradation, leading to bacterial lysis (12). From the screen, a 1-amino substituted tetrahydrocarbazole (THCz) hit class was identified that was found to be bactericidal at low micromolar concentrations. Comprehensive structure–activity relationship (SAR) studies of a series of synthesized THCz analogs identified the two central amine groups as essential for antibacterial activity. Mode of action studies revealed that THCz simultaneously inhibit different cell envelope biosynthesis pathways by targeting lipid II (peptidoglycan), lipid III_{WTA} (wall teichoic acid), and lipid I_{cap} (capsule) as well as the central lipid carrier undecaprenyl pyrophosphate (C_{55}-PP). Compared to natural lipid II inhibitors, THCz are relatively easy to synthesize and modify, and thus represent promising scaffolds for antibiotic drug development.

Results

Screening for Cell Wall Inhibitors. A whole-cell high-throughput screening (HTS) procedure was developed using the major respiratory tract pathogen *Streptococcus pneumoniae* as the bacterial target organism. The screen utilized the induction of pneumococcal autolysis to score for compounds with potential cell wall synthesis inhibiting activity. The decrease in optical density (OD_{600nm}) following compound treatment was used as an indicator of bactericidal activity and provided an easy and powerful readout for hit selection. For the main screen, we used the nonencapsulated strain Tigr4R (T4R) that is generally more sensitive to most treatments than the encapsulated

parental Tigr4 (T4) strain (Fig. 1*A*). Bacterial cultures in the early logarithmic growth phase were challenged with a compound library (50 μM per substance) comprising 17,500 substances (http://www.cbcs.se/), and the OD_{600nm} was measured at timed intervals. For 99.1% of the compounds, an increase in OD_{600nm} following compound addition was recorded, suggesting that no substantial growth inhibition occurred. Furthermore, no compound had a ΔOD_{600nm} value near zero at 120 min after challenge that would indicate bacteriostatic activity. Compounds yielding a negative ΔOD_{600nm} value at 120 min after treatment (156 compounds, 0.9%) were scored as hits. Out of these compounds, 71 also exhibited comparable activity against the encapsulated T4 strain and were validated on the LytA-deficient T4 derivative strain, resulting in a hit rate of 0. 4% for the total screen (Fig. 1*A*).

Characterization of THCz Analogs. The present study characterizes three hit compounds from the screen (THCz-1, THCz-2, and THCz-3) (Fig. 1*A*) and related synthesized derivatives. These initial THCz screening hits shared a central tetrahydrocarbazole scaffold with a short 1-amino substituted linker (–NH–CH_2CH_2–) and had different substitutions in positions R^1 and R^2 (Fig. 1). The minimum inhibitory concentration (MIC) of the hit compounds against *S. pneumoniae* was determined to 1 μg/mL (Tables 1 and 2 and *SI Appendix*, Tables S1–S3). Clinical pneumococcal isolates from the Pneumococcal Molecular Epidemiology Network strain collection, resistant to one or several conventional antibiotics, were equally as sensitive to THCz-1 as the wild-type strain (*SI Appendix*, Table S4), showing that common acquired resistance mechanisms did not confer decreased sensitivity to THCz-1. Further testing of THCz-1 against a panel of clinically relevant pathogens (Table 1) revealed antimicrobial activity against a broad range of gram-positive bacteria,
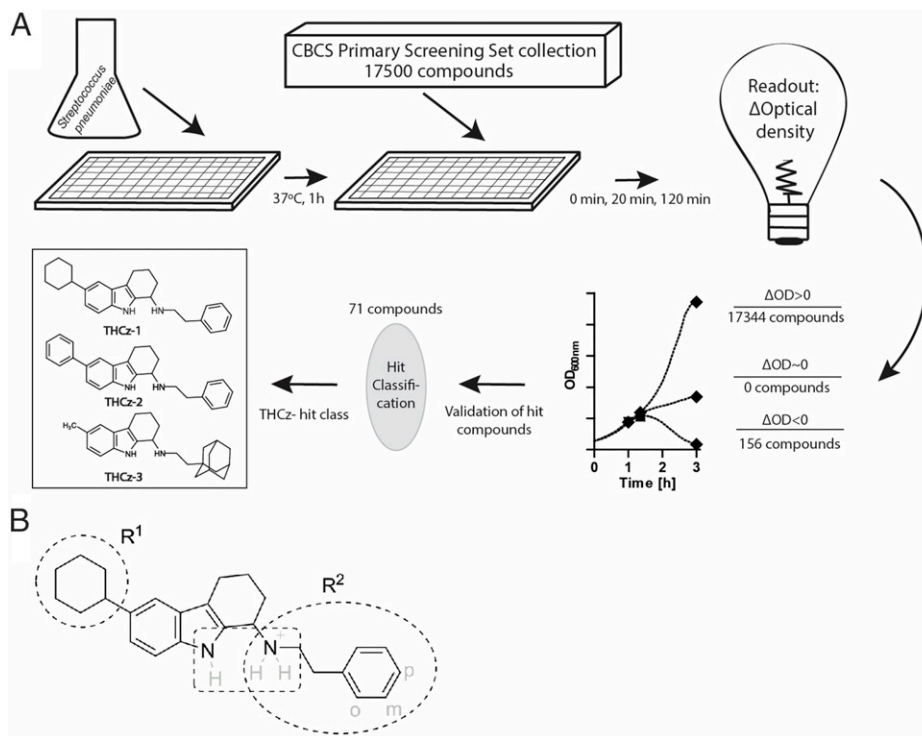
Fig. 1. Autolysin-mediated lysis screening identified THCz as an antibacterial hit class. (*A*) Schematic illustration of the autolysin-mediated lysis screen. Pneumococcal cultures grown in multiwell plates were challenged with the chemical compound library, and OD was recorded and used for evaluation of lysis induction and hit selection. Hit compounds were validated and classified. The three hit compounds from the tetrahydrocarbazole compound class (THCz-1, THCz-2, and THCz-3) are depicted. (*B*) Structure of THCz-1, where molecular moieties relevant for the structure activity and toxicity relationship investigations (R^1 and R^2) are highlighted with dashed lines. Also indicated is the central diamino motif that was identified as essential for activity shown in the protonation state likely encountered at physiological pH.

Table 1. Antibacterial spectrum of THCz-1

Species	Strain	MIC THCz-1, μg mL^{-1}
S. pneumoniae	T4	1*
		0.3†
Streptococcus parasanguinis	ATCC 903	5†
Streptococcus pyogenes	serotype M1T1 (45)	1†
B. subtilis	ATCC 6051	3†
	168	2
Staphylococcus simulans	22	2
Staphylococcus epidermidis	CLB26329 (MRSE)	2
S. aureus	ATCC 25923	5†
	ATCC 29213	2
	SG511	2
	USA300 JE2 (MRSA)	4
	SG511 DAP^R	2
	HG001	4
	HG001 DAP^R	4
	Mu50 (VISA)	2
	Vc40 (VISA)	4
	SA113	4
	SA113Δ*atlA*	4
	SA113Δ*tarO*	4
Enterococcus faecalis	JH2-2	2
E. faecium	BM4147 (VRE)	2
Micrococcus luteus	DSM1790	1
M. bovis	ATCC 35734	16‡
M. smegmatis	ATCC 70084	8‡
M. catarrhalis	ATCC 43617	1
E. coli	ATCC 11775	>41†
	O-19592	>128
	MB5746§	2
P. aeruginosa	ATCC 10145	>41†
N. gonorrhoeae		1 to 8¶

THCz-1 sensitivity was determined in cation-adjusted MHB. All strains are characterized in *SI Appendix*, Table S8.
*THCz-1 sensitivity was determined in supplemented C+Y medium.
†THCz-1 sensitivity was determined in THY medium.
‡THCz-1 sensitivity was determined in Tween80 supplemented cation-adjusted MHB.
§Outer membrane hyperpermeable and efflux deficient.
¶Depending on the medium.

including drug-resistant strains, such as methicillin-resistant *Staphylococcus aureus* (MRSA), vancomycin-intermediate *S. aureus* (VISA), and vancomycin-resistant *Enterococcus faecium* (VRE). Importantly, THCz-1 was also active against gram-negative pathogens such as *Neisseria gonorrhoeae* and *Moraxella catarrhalis,* with MIC values in the range of 1 μg/mL to 8 μg/mL, and against mycobacteria (*Mycobacterium bovis* and *Mycobacterium smegmatis*, 8 μg/mL to 16 μg/mL). Moreover, the substance displayed activity against an *Escherichia coli* strain with a defective outer membrane, but not against wild-type *E. coli* or *Pseudomonas aeruginosa,* indicating that the outer membrane of certain gram-negative species may provide protection against THCz-1. Interestingly, Su et al. (13) have previously recorded activity against an *E. coli* strain of a related THCz analog but with a 2,4-diaminopyrimidine substituent in position R^2.

As the hit compound THCz-1 was obtained from an HTS assay that employed pneumococcal autolysis as the readout, lysis and killing kinetics were compared to penicillin and tetracycline that inhibits peptidoglycan and protein synthesis, respectively. Treatment of pneumococci with THCz-1 induced a more rapid bacteriolytic effect than penicillin, and no viable colonies could be recorded 9 h after treatment (Fig. 2 *A* and *B*
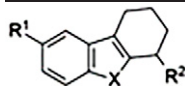
and *SI Appendix*, Fig. S1). The contribution of cell wall hydrolase activity to the lytic and bactericidal response was assayed using an isogenic pneumococcal strain deficient in the major autolysin LytA (T4Δ*lytA*) grown in an elevated (110 mM) concentration of choline chloride that causes cell wall dissociation and functional inactivation of other choline-binding cell wall hydrolases. In the absence of hydrolase activity, reduced lysis was observed following treatment of pneumococci with THCz-1 and penicillin (Fig. 2*C*), yet the bactericidal effect was retained, albeit with delay (Fig. 2 *B* and *D*). Tetracycline caused a growth-inhibitory phenotype without any prominent lysis and displayed a considerably slower killing curve that was not affected by the activity of cell wall hydrolases (Fig. 2 *A–D*). Transmission electron microscopy (TEM) of THCz-1–treated unencapsulated T4R cells confirmed that lysis was exerted through the action of choline-binding cell wall hydrolases, since bacteria remained intact in a strain lacking the major autolysin *lytA* (T4RΔ*lytA*) grown in elevated choline chloride concentration (Fig. 2 *E–H*). THCz-1–treated *S. pneumoniae* (T4R) displayed cell wall ruptures in close proximity to the equatorial plane (Fig. 2*F*) correlating to the site where nascent peptidoglycan, the putative substrate of LytA, has been suggested to be incorporated during cell wall synthesis (14, 15). Together, these data confirmed that THCz-1 treatment, as for penicillin, caused induction of autolysin-mediated lysis, although the bactericidal activity is not solely explained by autolysin activation.

SAR. We next explored the molecular context of the THCz compound class in relation to the antibacterial activity. For this, we developed a synthesis scheme for substituted THCz and oxygen analogs (*SI Appendix*, Figs. S2 and S3) that allowed an exploration of the SAR of THCz derivatives and the investigation of the impact on toxicity of different substitutions on cultured human cell lines. The following SAR description is supported by a more extensive analysis provided in *SI Appendix*, Tables S1–S3, Fig. S4, and *SI Text*. The central diamino motif (Fig. 1*B*) was found to have a major impact on the antibacterial activity (*SI Appendix*, Table S1). Thus, replacement of either of the two nitrogens with oxygens of otherwise similar analogs led to no, or much reduced, antibacterial activity (THCz-2 vs. THCz-6 and THCz-5 vs. THCz-19) (Table 2). However, also, the cytotoxic properties of THCz analogs were correlated to the presence of the diamino motif, as the 50% inhibitory concentration (IC$_{50}$) increased about sixfold for THCz-5 vs. THCz-19, and about sevenfold for THCz-6 vs. THCz-2 (Table 2).

Further investigation of the effect of substitutions in position R^1 and R^2 of the THCz scaffold was performed (Fig. 1*B* and *SI Appendix*, Tables S1–S3). Most substitutions in position R^1 had little or no effect on the antibacterial activity, and an unsubstituted analog (THCz-45) maintained activity. However, a carboxylate in R^1 (THCz-42) was found to have a marked negative effect on the antibacterial activity, suggesting that an anionic substituent in this position was not suitable. Sterically demanding substituents in R^1 (THCz-43 and THCz-44) did have an adverse effect on toxicity, leaving a methyl group (i.e., THCz-39 and THCz-40) or an unsubstituted R^1 (THCz-19 and THCz-45) the most favorable of the herein tested R^1 substitutions. In position R^2, it was important for antibacterial activity that a sterically demanding substituent, such as an adamantyl or a phenyl (i.e., THCz-3 and THCz-36 vs. THCz-24), was linked to the central scaffold by at least two carbons (THCz-36, THCz-37, and THCz-38 vs. THCz-35). Substitutions in the phenyl ring of R^2 were only favorable in the *para* position in the context of toxicity. A hydroxyl or bromo substituent (THCz-39 and THCz-40) caused a twofold to fourfold reduction in MIC and a corresponding increase in IC$_{50}$ in comparison to the original screening hit THCz-1 (Table 2).

Table 2. SAR and toxicity of a selection of THCz analogs

THCz-	R1*	X	R2*	MIC [μM (μg mL⁻¹)][†]	IC₅₀ [μM(μg mL⁻¹)] [n][‡]
1[§]	cyclohexyl	NH	phenethyl-NH	3.1 (1.3)	12.1 (4.9) ± 3.0 (1.2) [6]
2[§]	phenyl	NH	phenethyl-NH	3.1 (1.1)	17.5 (7.1) ± 1.9 (0.8) [3]
5	H	NH	phenethyl-O	>100 (>29.1)	140.8 (41.0) ± 16.9 (4.9) [4]
6[¶]	phenyl	O	phenethyl-NH	50 (18.4)	134.1 (49.3) ± 42.4 (15.6) [5]
19	H	NH	phenethyl-NH	6.3 (1.9)	22.2 (6.8) ± 1.8 (0.6) [3]
39	Me	NH	OH-phenethyl-NH	6.3 - 12.5 (2.0 - 4.0)	33.4 (10.7) ± 5.9 (1.9) [7]
40	Me	NH	Br-phenethyl-NH	6.3 (2.4)	28.0 (10.7) ± 4.1 (1.6) [7]

*Cy, cyclohexyl; Ph, phenyl; Me , methyl.
[†]Minimal inhibitory concentration of THCz analogs for *S. pneumoniae* T4 in supplemented C+Y medium. Most abundant MIC is given. An overview of the observed MIC distribution is given in *SI Appendix*, Fig. S4.
[‡]IC₅₀ values of 10^5 A549 cells/mL challenged with a serial titration of the respective THCz analogs. Average ± SD are given, and the number of biological replicates is noted in brackets. In the presence of 10% fetal bovine serum, mimicking cell culture conditions, the plasma protein binding affinity of THCz analogs caused an overall fourfold increase in MIC (*SI Appendix, SI Text*).
[§]Original hit compounds from the screen; see also Fig. 1 for structures.
[¶]For simplicity, we refer to all compounds studied here as THCz, although this compound is an oxa-tetrahydrofluorene.

The THCz analogs contain a stereocenter (*SI Appendix*, Fig. S5 *A* and *B*), and the initial screen and the SAR were carried out with racemic mixtures of the two enantiomers. We therefore separated the enantiomers from a subset of THCz analogs (THCz-1, THCz-39, and THCz-40) (*SI Appendix*, Fig. S5 *C–I*) and tested their antibacterial activities separately. Our data showed that both the R and S forms displayed similar MIC (*SI Appendix*, Table S5) in comparison to each other and to the racemic mixture. Combined, the untargeted investigation on modifications of the THCz scaffold showed that the central diamino motif was essential, and sterically demanding substitutions on a not less than two-carbon chain linker in R^2 were required, while modifications in R^1 were dispensable for antibacterial activity.

Mode of Action Studies. As THCz analogs showed an autolysin-inducing bacteriolytic effect in the early logarithmic phase, a well-known feature for cell wall targeting agents, we reasoned that THCz might interfere with cell wall synthesis. To verify this hypothesis and to approach target identification, a set of pathway-specific *Bacillus subtilis* bioreporter strains (16, 17) was treated with selected active analogs, THCz-1, THCz-39, and THCz-40 and compared to the inactive derivative THCz-5 (Table 2 and *SI Appendix*, Table S5). Indeed, THCz-1, THCz-39, and THCz-40, but not THCz-5, specifically induced the cell wall responsive reporter strain, while reporter strains indicative for interference with DNA, RNA, and protein biosynthesis were not activated (Fig. 3*A*). Furthermore, treatment of *B. subtilis* with

THCz-1, THCz-39, and THCz-40 induced characteristic cell shape deformations, as visualized through phase-contrast microscopy, revealing the formation of cell membrane blebbing, indicative of inhibition of peptidoglycan biosynthesis and autolysin activation. Membrane blebbing was also observed following control treatment with vancomycin, nisin, or bacitracin, but not with the inactive THCz-5 or with antibiotics having targets other than the cell wall, such as clindamycin, ciprofloxacin, and rifampicin (Fig. 3*B*). To narrow down the target within the peptidoglycan biosynthesis pathway, we investigated the effect of THCz analogs on the LiaRS stress response using a *B. subtilis* luciferase bioreporter. The LiaRS two-component system is known to be sensitively induced in response to antibiotics that target lipid II or C₅₅-PP, for example, vancomycin or bacitracin (18). Monitoring P$_{liaI-lux}$ bioluminescence over time revealed a strong induction for all THCz analogs tested, except for the inactive analog THCz-5 (Fig. 3*C*). Similar induction of the LiaRS reporter was also observed for the separated enantiomers of the active analogs, validating that the S and R forms have the same mode of action (*SI Appendix*, Fig. S6 *A–C*).

Corroborating interference with the lipid II biosynthesis cycle, treatment of *S. aureus* whole cells resulted in accumulation of the ultimate soluble peptidoglycan precursor UDP-MurNAc-pentapeptide (Fig. 3*D*), indicating that a late-stage membrane-associated peptidoglycan biosynthesis step was inhibited. Higher THCz concentrations (>5× MIC) impeded cytoplasmic accumulation due to increased lysis, as a result of induction of the autolytic system, or due to effects related to membrane interaction.
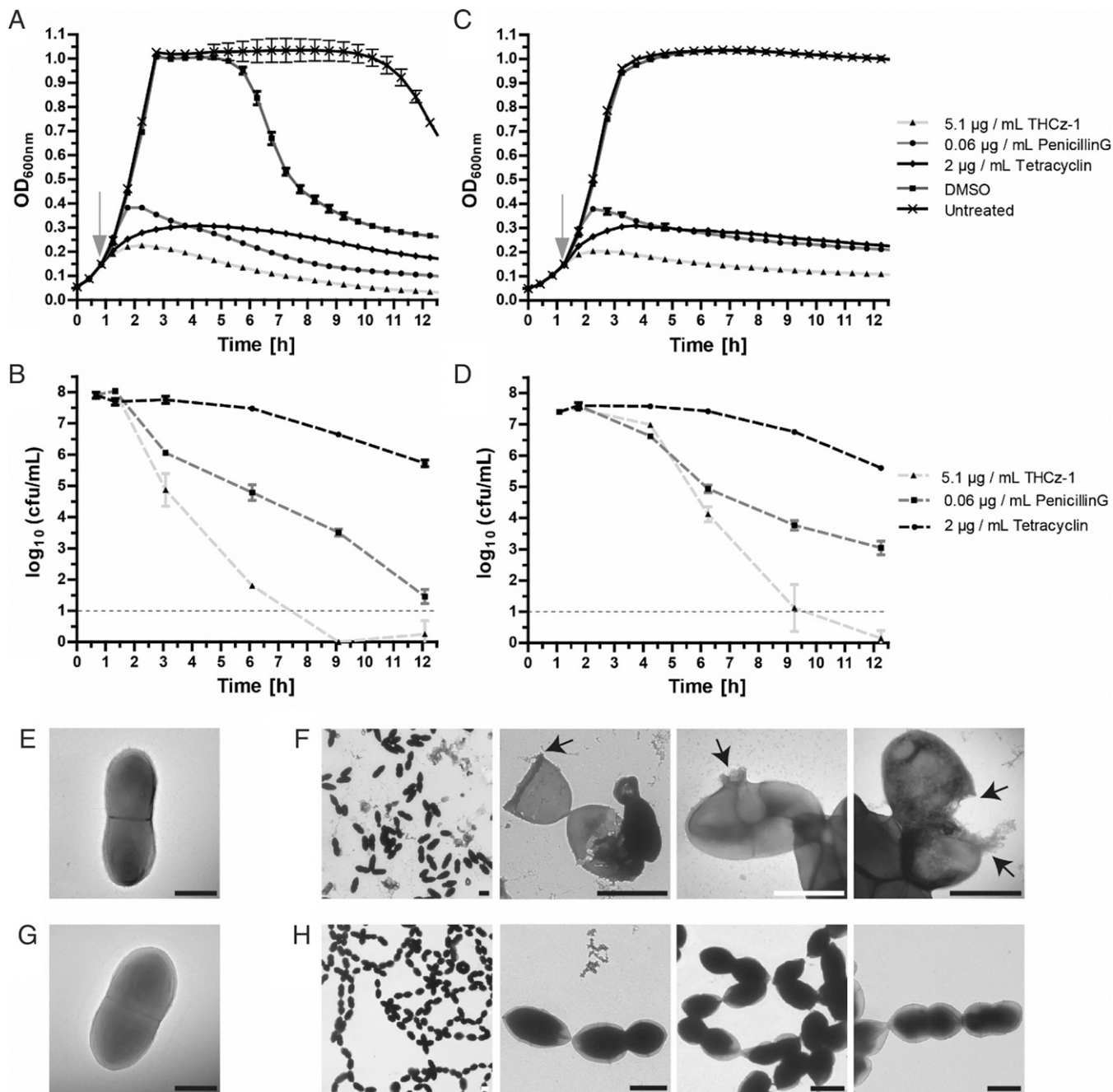
Fig. 2. Kinetics of pneumococcal lysis and viability following THCz-1 treatment. Treatment of (*A* and *B*) T4 wild type and (*C* and *D*) T4Δ*lytA* with THCz-1 (5.1 µg/mL, 12.5 µM, 4× MIC), penicillin G (0.06 µg/mL, 2× to 4× MIC), tetracycline (2 µg/mL, 8× to 16× MIC), or (in *A* and *C*) DMSO (1%). Bacteria were grown in C+Y media in the absence (*A* and *B*) or presence (*C* and *D*) of 110 mM choline chloride that inhibits cell wall association of autolysins and cell wall hydrolases of *S. pneumoniae*. Dotted black lines in *B* and *D* indicate the detection limit of the assay. Growth kinetics (*A* and *C*) are shown from one representative experiment as the average and SD of three technical replicates. Death kinetics (*B* and *D*) are summarized as the average and SD of three independent experiments. Short dashed black lines in *B* and *D* indicate the detection limit of the assay. (*E*–*H*) Electron micrographs of T4R (*E* and *F*) and T4RΔ*lytA* (*G* and *H*), fixed and imaged after treatment with THCz-1 (25 µM) (*F* and *H*) and as untreated controls (*E* and *G*). In *F* and *H*, representative overview images of cell populations are shown (*Left*) followed by three close-up images (*Right*). The use of unencapsulated mutants facilitated examination of the cell morphology. Pneumococcal chain formation in choline-treated autolysin-deficient T4RΔ*lytA* cells are attributable to the inhibition of LytB activity, required for separation of diplococcal cells (44). (Scale bars, 1 µm.)

THCz did not induce the formation of pores in comparison to the lantibiotic nisin which is an established pore former (*SI Appendix, Supplementary Materials and Methods* and Fig. S7)(9). However, THCz treatment resulted in the delocalization of GFP-MinD in *B. subtilis*, indicating membrane depolarization. The cell division inhibitor MinD is bound to the membrane via a

C-terminal amphipathic helix and requires the presence of the membrane potential for its specific cellular localization pattern. MinD localizes to newly formed cell poles, thereby directing FtsZ to midcell guiding division septum placement (19). Compared to untreated control cells, GFP-MinD delocalized in cells treated with THCz, resulting in irregular dispersion of GFP-MinD within
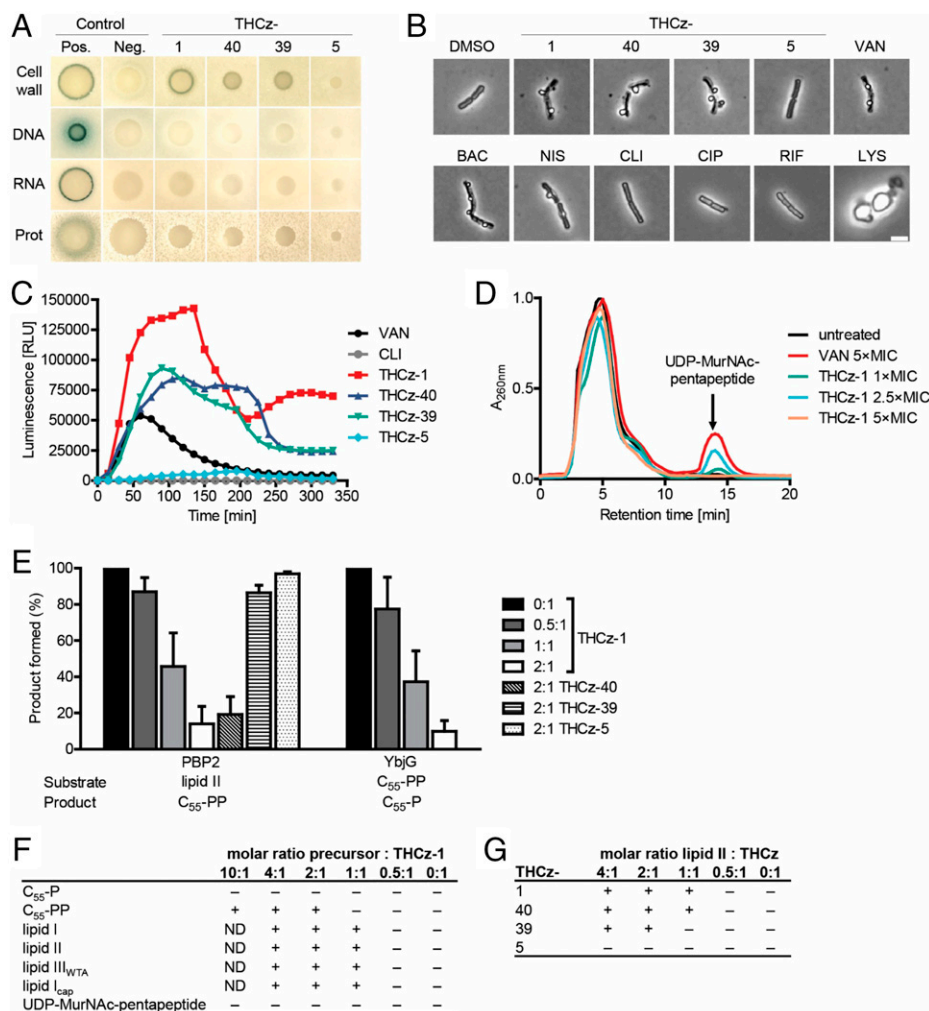
Reithuber et al.
THCz: Small molecules with antimicrobial activity that block cell wall lipid intermediates

PNAS | 5 of 12
https://doi.org/10.1073/pnas.2108244118

Fig. 3. THCz analogs with intact diamino motif interact with C_{55}-PP and C_{55}-PP–linked cell wall precursors. (*A*) Impact of THCz-1 and analogs (THCz-40, THCz-39, and THCz-5) on major biosynthesis pathways in *B. subtilis*. *B. subtilis* bioreporter strains with selected promotor-*lacZ* gene fusions were used to identify interference with DNA (P_{yorB}), RNA (P_{yvgS}), protein (P_{yhel}), and cell wall (P_{ypuA}) biosynthesis. Induction of a specific stress response results in expression of β-galactosidase indicated by a blue halo surrounding the inhibition zone. Antibiotics vancomycin, ciprofloxacin, clindamycin, and rifampicin were used as positive controls. (*B*) Treatment of *B. subtilis* with THCz induces severe cell shape deformations as visualized by phase-contrast microscopy. (Scale bar for all images: 2 μm.) (*C*) Induction of the LiaRS bioreporter by THCz compared to vancomycin, indicating interference with the lipid II biosynthesis cycle. (*D*) Intracellular accumulation of the ultimate soluble cell wall precursor UDP-MurNAc-pentapeptide in vancomycin-treated and THCz-1–treated cells of *S. aureus* as analyzed by means of reverse-phase HPLC. (*E*) Impact of THCz on individual peptidoglycan biosynthesis reactions. THCz inhibits the PBP2-catalyzed transglycosylation of lipid II and the YbjG-catalyzed dephosphorylation of C_{55}-PP. THCz were added in molar ratios of 0.5 to 2 with respect to the amount of the substrate lipid II or C_{55}-PP used in the individual test system. Inhibitions of PBP2- and YbjG-catalyzed reactions were quantified by the relative amount formed of C_{55}-PP and C_{55}-P, respectively. The error bars represent the SD from the triplicate runs. (*F* and *G*) Antagonistic effect of purified cell wall intermediates on antimicrobial activity of THCz. THCz compounds were exposed to selected purified cell wall precursors for 10 min at indicated molar ratios prior to incubation with *M. luteus* cells; +, antagonization of antimicrobial activity; −, no antagonization; ND, not determined. Results of three independent experiments are shown.

5 min. MinD delocalization was also observed for the inactive THCz-5 variant, suggesting that the induced membrane effects are not the primary cause of killing (*SI Appendix*, Fig. S8).

In search of the molecular target, we next investigated the impact of THCz-1 on peptidoglycan biosynthesis reactions in vitro using purified *S. aureus* enzymes and substrates. Quantitative analysis of PBP2-mediated transglycosylation of lipid II revealed a dose-dependent inhibition (Fig. 3*E*). Almost complete inhibition was observed at a twofold molar excess of THCz-1 with respect to lipid II, suggesting that THCz-1 forms a stoichiometric complex with the substrate rather than inhibiting the enzyme. Similarly, lipid II synthesis catalyzed by the MurG glycosyltransferase was inhibited (*SI Appendix*, Fig. S9). Furthermore, THCz-1 was also found to inhibit dephosphorylation of C_{55}-PP to C_{55}-P, a crucial step in the recycling of the

lipid carrier conducted by undecaprenyl pyrophosphate phosphatase YbjG. A twofold molar excess of THCz-1 caused a full inhibition of YbjG-mediated dephosphorylation of C_{55}-PP (Fig. 3*E*). Corroborating, the addition of purified C_{55}-PP, lipid I and lipid II as well as the wall teichoic acid precursor lipid III_{WTA} (C_{55}-PP-GlcNAc) and the capsular precursor lipid I_{cap} (C_{55}-PP-glucose) all antagonized the antimicrobial activity of THCz-1, while C_{55}-P did not (Fig. 3*F*). These data thus clearly indicate that THCz-1 interacts with undecaprenyl pyrophosphate and C_{55}-PP–containing cell wall precursors. However, the interaction with the first sugar moiety attached to the lipid carrier appears to contribute to binding, since a higher concentration of C_{55}-PP than of lipids I, II, and III_{WTA} and lipid I_{cap} was required to fully antagonize THCz-1 activity (Fig. 3*F*). Furthermore, lipid II was found to antagonize THCz analogs

THCz-39 and THCz-40 that contained an intact diamino motif, in contrast to the inactive THCz-5 (Fig. 3G). In accordance with the in vitro data and the SAR profile, THCz-39 was less efficiently antagonized by lipid II compared to THCz-1 and THCz-40 (Fig. 3G), and fourfold higher concentrations of THCz-39 were required for full inhibition of the PBP2-catalyzed reaction (*SI Appendix*, Fig. S10). In agreement with the in vitro activity of the racemic mixture, both enantiomers of THCz-40 similarly inhibited lipid II transglycosylation (*SI Appendix*, Fig. S6 *D and E*). Combined, these data indicate that the pyrophosphate moiety represents the essential motif for target interaction, and that the diamino motif of THCz analogs is required for this interaction. In agreement, the MurT/GatD-catalyzed amidation of lipid II was unaffected in the presence of THCz-1, strongly suggesting that the stem peptide of lipid II is not involved in binding (*SI Appendix*, Fig. S11). Furthermore, THCz analogs did not interfere with the PBP4-mediated carboxypeptidation, releasing the terminal D-Ala residue from the pentapeptide stem (*SI Appendix*, Fig. S9B), suggesting that interactions with the lipid II stem peptide are less relevant and that THCz do not sterically hinder enzyme interaction with that region of the target molecule. Compared to natural lipid II binders, for example, vancomycin, THCz do not form extraction-stable complexes with lipid II (*SI Appendix,* Fig. S12), pointing to decreased binding affinity.

Together, these data reveal that THCz specifically binds to multiple undecaprenyl pyrophosphate–coupled cell wall precursors, and with C_{55}-PP as such, thereby simultaneously inhibiting several cell wall biosynthetic pathways, including the recycling of the C_{55}-P carrier utilized by all these pathways.

A recent study reported that fungal P-type ATPases can be inhibited by similar THCz analogs, and a complex with a THCz analog and a mammalian Ca^{2+} ATPase (SERCA) was shown in a cocrystal structure (20). However, in our study, neither single-deletion mutants of the four genes annotated as P-type ATPases in the *S. pneumoniae* T4 strain (*SP0729, SP1551, SP1623,* and *SP2101*) (*SI Appendix*, Tables S7 and S8) nor the quadruple mutant displayed decreased sensitivity to THCz-1, suggesting that P-type ATPases are not essential bacterial, or at least pneumococcal, THCz targets (*SI Appendix*, Table S6). The sequence similarity of these pneumococcal P-type ATPases with rabbit/human SERCA is only between 21% and 38% by identity, suggesting that the binding interfaces might be different.

THCz-1 Affects Capsule Production. More recently, dual targeting of similar cell wall precursors by teixobactin was correlated with a limited propensity to develop resistance (5). Resistance to THCz-1 also did not readily develop in vitro, as no resistant mutants were obtained when continuously subculturing *S. aureus* using a broth microdilution method with sublethal concentrations of THCz-1 (*SI Appendix, Supplementary Materials and Methods* and Fig. S13). However, through continuous cultivation of encapsulated *S. pneumoniae* T4 on THY plates containing small incremental concentrations of THCz-1, we could obtain an isolate (#22) with marginally decreased sensitivity to THCz-1 compared to control strains similarly passaged on THCz-1–free THY plates (BHN1368-9). Comparative sensitivity testing in THY liquid medium confirmed that, even though clone BHN1364 of the continuously THCz-1 exposed isolate #22 was affected by 2× MIC, it could still grow at this concentration, contrary to the unexposed clone BHN1368, which tolerated only 1× MIC (Fig. 4 *A* and *B*). Whole genome sequencing of four #22 derived clones (BHN1364-7) identified a set of point mutations that were absent in the control strains (*SI Appendix, Supplementary Materials and Methods and Fig. S14*). Thus, we constructed deletion mutants in the corresponding genes (*cpsE* (BHN1690), *aguA* (BHN1371), pneumolysin (*ply*) (BHN2043), and *SP1901* (BHN1693) (*SI Appendix, Supplementary Materials and Methods* and Tables S7 and S8).

Only a deletion mutant of *cpsE* (BHN1690), as well as the strain with the reconstituted nonsynonymous mutation *cpsE*[G394C] (BHN1691), displayed a similar decrease in sensitivity. Pneumococcal *cpsE* encodes the glycosyltransferase that adds a sugar phosphate to the C_{55}-P lipid carrier to initiate capsule synthesis in the cytoplasm and is therefore essential for biosynthesis of the polysaccharide capsule, which is the main virulence factor for pneumococci (21, 22). Indeed, the *cpsE*[G394C] mutant was found to express lower amounts of capsular polysaccharide in comparison to wild-type T4 but was not deficient in capsule production, similar to the T4Δ*cpsE* strain (Fig. 4C). The influence of capsule expression on THCz-1 sensitivity was supported by the reduced THCz-1 sensitivity observed in the capsule-deficient T4R strain (*SI Appendix*, Table S8), that was found refractory to even 2.4× MIC THCz-1 (Fig. 4D). This increased sensitivity to THCz-1 mediated by pneumococcal capsular expression was already apparent after 1 h of exposure to a 2× MIC concentration of THCz-1, where the encapsulated T4 was killed more prominently than the unencapsulated T4R and marginally more than the less encapsulated T4*cpsE*[G394C]-Erm (BHN1691) (Fig. 4E). Thus, decreased or abolished capsule production caused a marginal desensitization to THCz-1. Interestingly, a short passage of *S. pneumoniae* in sub-MIC concentrations of THCz-1 (*SI Appendix, Supplementary Materials and Methods*) led to a decrease in the phosphorylcholine amount compared to the untreated strains (*SI Appendix, Supplementary Materials and Methods* and Fig. S15)as well as a decrease in the sensitivity of T4Δ*lytA* to externally added LytA (*SI Appendix, Supplementary Materials and Methods* and Fig. S16), indicating that THCz-1 also targets teichoic acid synthesis.

Discussion

In the present study, we developed a screening procedure where small-molecular compounds were screened for their ability to trigger autolysin-mediated lysis of pneumococci in order to find potential cell wall inhibitors. Although discovered in the 1970s, the underlying molecular mechanisms behind how cell wall–targeting antibiotics trigger autolysin activation still remain elusive (12). It has been suggested that an active cell wall synthesis machinery would sequester a potential autolysin substrate and that autolysin misplacement on teichoic acids would be part of the triggering event (14, 23–27). Our screening procedure for pneumococcal autolysin activation provided an uncomplicated and powerful protocol for identification of potential cell wall inhibitors. The herein described THCz compound class was one of the most active identified in the screen. Related THCz analogs with antimicrobial activity have been reported, but few targets have been proposed (13, 20, 28). Our mode of action studies revealed that THCz analogs stalled cell wall biosynthesis by targeting lipid II and other undecaprenyl pyrophosphate–containing lipid precursors involved in teichoic acid and capsule synthesis. The interaction required the pyrophosphate moiety (C_{55}-PP) as minimal motif, and THCz relied on the diamino motif for potent antibacterial activity. It seems therefore likely that the two amino groups of THCz interact with the two negatively charged phosphate groups of the target. Supporting this, THCz analogs are expected to be positively charged at physiological pH, since the amino group in R^2 has a calculated pK_a of 9.8 (for THCz-1). Furthermore, the requirement of a –NH–CH_2CH_2– linker-connected hydrophobic group in position R^2 supports a model for target interaction in which this group is inserted into the plasma membrane to facilitate the diamino–pyrophosphate interaction (Fig. 5). The comparable activities of the tested THCz enantiomers could possibly be understood by such a model. If the role of the hydrophobic part of R^2 is to anchor THCz into the plasma membrane, the relative stereo conformation would not be crucial for the
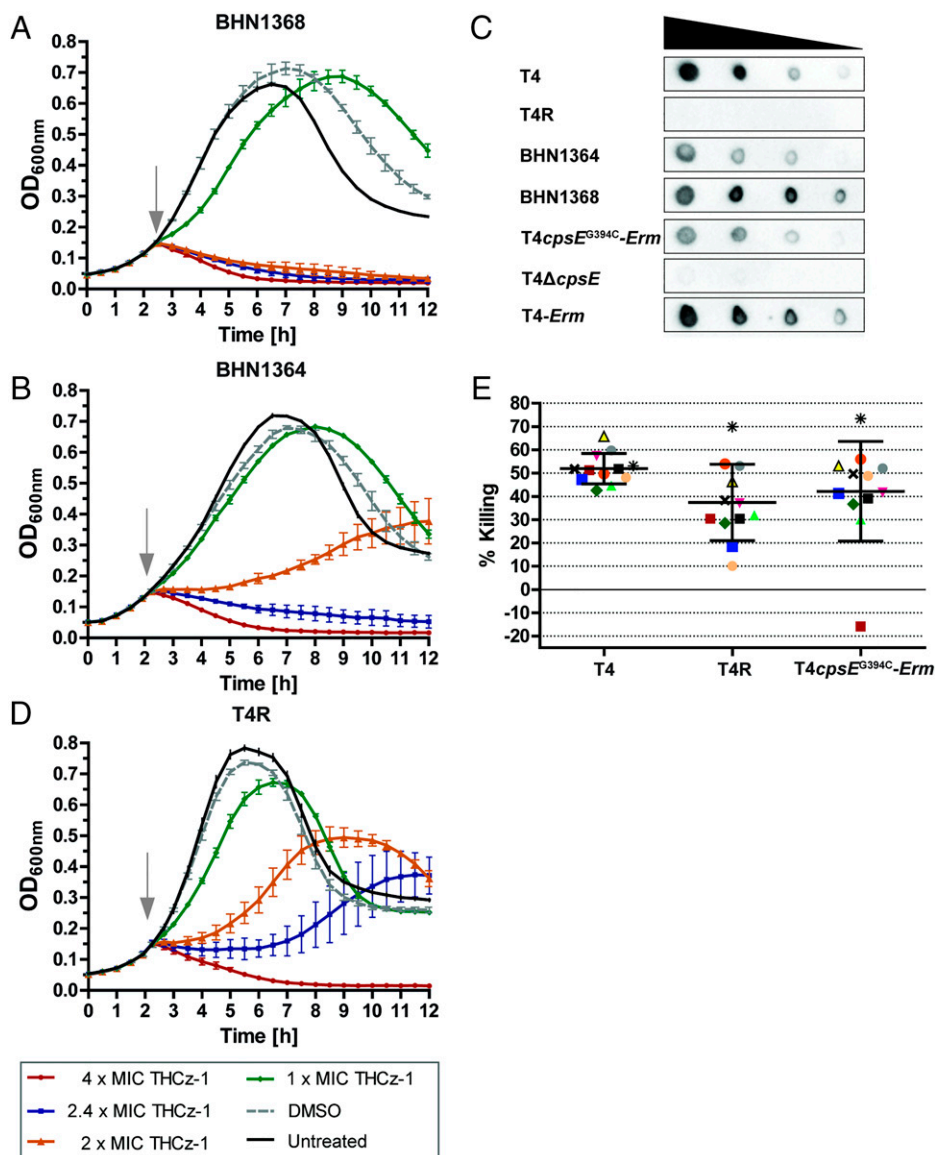
Fig. 4. Decreased capsular polysaccharide production confers reduced sensitivity to THCz. Growth curves of strains (*A*) BHN1368 and (*B*) BHN1364 in THY medium challenged with a titration series of THCz-1, solvent control (DMSO) in comparison to untreated growth control. (*C*) Quantification of the capsular polysaccharide amount of the wild-type T4 (BHN842), the unencapsulated T4R (BHN659), an isolate of T4 with reduced THCz-1 sensitivity (BHN1364), unexposed control strain of T4 with retained THCz-1 sensitivity (BHN1368), point mutant T4*cps4E*^{G394C}-erm (BHN1691) with an *erm* open reading frame (ORF) inserted in the capsular operon after *cps4E* ORF, the *cpsE* knockout strain (BHN1690), and the control wild-type strain T4-erm(BHN1692) with an *erm* ORF inserted in the capsular operon after *cps4E* ORF. (*D*) Growth curve and exposure to a serial dilution of THCz-1 of T4R. (*E*) Bacterial killing after 1 h of exposure to 2× MIC THCz-1 (1.5 μM, 0.6 μg/mL in THY medium) of wild-type T4 (BHN842), the unencapsulated T4R (BHN659), and the mutant T4*cpsE*^{G394C} (BHN1691). Paired experiments (each experiment was carried out in technical triplicates) are depicted with the same symbol. Average and SD are given.

diamino–pyrophosphate interaction. This would thus contrast many antibiotics where stereoisomers display stereoselectivity due to protein binding constraints (29).

THCz analogs displayed a broad antibacterial spectrum and were active against all gram-positive Firmicutes species tested as well as Actinobacteria, including mycobacterial species. Notably, they were also active against gram-negative *N. gonorrhoeae* and *M. catarrhalis*, possessing lipooligosaccharides instead of lipopolysaccharides, which provides higher permeability across the outer membrane (30, 31), as has been observed for cationic and amphiphilic antimicrobial peptides, for example, the defensin Plectasin and the lantibiotic nisin (32). This is probably attributable to their relatively small molecular mass that allows for translocation across the outer membrane of

certain species. THCz did not exhibit antimicrobial activity against wild-type *E. coli*, while an *E. coli* mutant with a hyper-permeable outer membrane was shown to be susceptible, indicating that THCz, despite their small size, are unable to pass the water-filled porins of gram-negatives. In addition to the broad antimicrobial spectrum, the low propensity of resistance development and absence of cross-protective resistant phenotypes are attributable to the target. The ubiquitous and highly conserved undecaprenyl pyrophosphate constitutes a keystone lipid scaffold for the synthesis and subcellular translocation not only of peptidoglycan but also for teichoic acids and polysaccharide capsule precursors, and is therefore hard for bacteria to modify. In accordance, the slightly decreased THCz-1 sensitivity of the obtained spontaneous *cpsE* mutant with decreased capsule
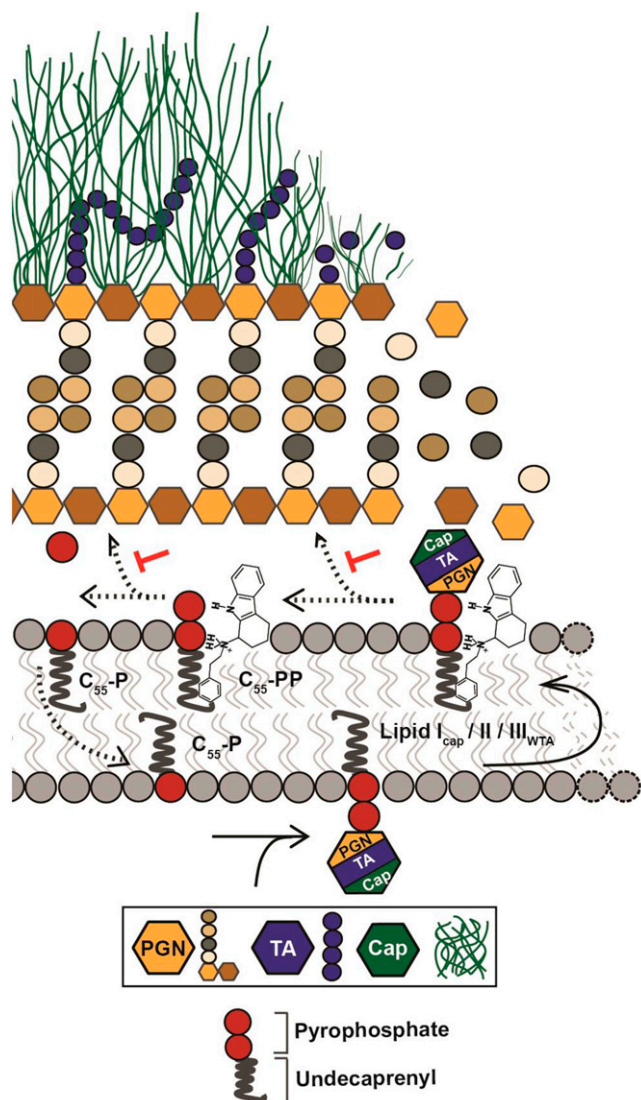
did not affect sensitivity to THCz-1, arguing against these proteins as antibacterial targets. The low sequence similarity (< 39%) between the pneumococcal and mammalian orthologs indicates that the binding interface might be different. Thus, knowledge of the structural requirements for C_{55}-PP interaction of THCz and the constrains of mammalian P-type ATPases binding should facilitate further modifications of THCz analogs to reduce cytotoxicity without affecting the antibacterial activity. In conclusion, the presented THCz analogs represent a class of small (<500 Da) synthetic molecules that inhibit bacterial cell wall synthesis by binding to lipid II and other undecaprenyl pyrophosphate–containing lipid precursors, targets conserved and present in all bacteria. This bacterial target interaction is highly attractive, and the small size and relative ease by which tetrahydrocarbazoles can be synthesized and modified could constitute a molecular platform for development of novel bacterial cell wall inhibitors.

Materials and Methods

Chemicals. A subset of 17,500 compounds from the Chemical Biology Consortium Sweden Primary Screening Set collection were screened in the whole-cell HTS assay. These compounds are chemically diverse and have lead- to drug-like properties with respect to parameters such as molecular weight, hydrogen bond accepting and donating groups, lipophilicity, and polar surface area. Compounds THCz-1, THCz-2, THCz-3, THCz-24, and THCz-35 corresponding to ChemBridge ID nos. 5279631, 5272685, 5265433, 5279631, and 5277652, respectively, were purchased from ChemBridge. All other compounds were synthesized as described in *SI Appendix* for general chemistry and synthesis of THCz analogs. The separation of enantiomers, circular dichroism spectroscopy, and the synthesis of the stereoselective compound (+)-(R)-AL682 are also given in *SI Appendix*. THCz analogs were dissolved in anhydrous dimethyl sulfoxide (DMSO) (Invitrogen).

Bacterial Growth Conditions. Pneumococci were cultured overnight on blood agar plates at 37 °C with 5% CO_2. For pneumococcal suspension cultures, C+Y medium (*SI Appendix*) supplemented with 9% Glucose Bouillon (1% glucose added to 25 g/L Nutrient broth No. 2, Oxoid) and 1% horse serum (Håtunalab) or Todd Hewitt broth (Sigma-Aldrich-T1438) with 0.5% yeast extract (THY medium) were used as indicated. For experiments with T4Δ*lytA* (*SI Appendix*, Table S8), the growth medium was supplemented with 110 mM choline chloride (Sigma), to inhibit choline-binding cell wall hydrolases. Growth conditions for other bacterial species are specified in the respective sections.

HTS Procedure. The unencapsulated *S. pneumoniae* strain T4R (*SI Appendix*, Table S8), an isogenic T4-derived strain, was used for the primary antibiotic screen. *S. pneumoniae* was grown in C+Y medium to an optical density at 600 nm $OD_{600nm} = 0.6$ and sedimented by centrifugation (5 min, 5,000 rcf, 4 °C). The cells were resuspended in a 1:10 volume (thus 10-fold concentrated) in C+Y medium containing 20% glycerol and frozen at −80 °C. For screening, a 0.5-mL aliquot was thawed and diluted by mixing with 49.5 mL of prewarmed (37 °C) C+Y medium. The bacterial suspension was distributed into 96-well tissue culture plates (200 μL per well) and incubated for 1 h at 37 °C. Screening compounds dissolved in DMSO at a concentration of 5 mM were added by the assistance of a pipetting robot (Beckman Coulter, Biomek NX^P) to a final concentration of 50 μM. The OD_{600nm} was measured immediately after compound addition ($t = 0$), after 20 min ($t = 20$), and after 2 h ($t = 120$). All calculations were done correlated to the OD measurement at $t = 0$ to take into account any possible contribution to the optical density from the compounds. Challenge with penicillin G (1 μg/mL) was used as positive control treatment, and DMSO (1% vol/vol) was used as a negative control treatment. Positive hits were scored as compounds that caused a Δ-negative OD_{600nm} measurement after 120 min following treatment [$Δ = OD_{600nm}(t = 0) − OD_{600nm}(t = 120)$]. Hits were validated on the encapsulated wild-type T4 and a T4 strain deficient in LytA (T4Δ*lytA*).

Lysis Kinetics. For comparative lysis kinetics precultures of T4 or T4Δ*lytA* grown in supplemented C+Y medium (with an additional 110 mM choline chloride for the autolysin mutant) to midlog phase [$OD_{600nm} ≈ 0.5$ (~5 to 6 × 10^8 colony-forming units (cfu)/mL)] were diluted to $OD_{600nm} = 0.05$ in fresh media and distributed into wells (400 μL per well) of a Honeycomb plate (Oy Growth Curves AB Ltd). A Bioscreen C plate reader (Oy Growth Curves AB Ltd) was used to record the growth kinetics. Cultures were grown to early log-phase ($OD_{600nm} ≈ 0.15$ (~1 to 2 × 10^8 cfu/mL), and treatments were added to a

Fig. 5. Proposed model for the mechanism of bactericidal action of THCz. Cell wall polymer precursors (lipid II, lipidIII$_{WTA}$, and lipid I$_{cap}$) are synthesized in the cytoplasm onto C_{55}-P to form C_{55}-PP–linked substrates that are flipped over to the outer leaflet of the plasma membrane to provide building blocks for peptidoglycan (PGN), teichoic acid (TA), or capsular (CAP) biosynthesis. Our data suggest that the pyrophosphate is the essential binding motif of THCz, presumably by electrostatic interaction, thereby stalling all three branches of cell wall polymer formation as well as dephosphorylation and recycling of C_{55}-PP to C_{55}-P.

production might have a liberated C_{55}-P pool that could, instead, be available for peptidoglycan and teichoic acid production. As capsule production is required for pneumococcal virulence, such mutants are likely attenuated in virulence.

THCz analogs, similar to those described here, have been shown to exhibit antifungal properties by binding to and inhibiting P-type ATPases (20). Related mammalian P-type ATPases such as the Ca^{2+}-ATPase (SERCA) were also inhibited by THCz analogs, and a cocrystal structure of a THCz analog and SERCA revealed the binding site. The binding is stabilized by interactions with the diamino motif of THCz via two aspartic acids (D59 and D254) (20). This is also in line with our data showing that THCz diamino motif is involved in toxicity, suggesting inhibition of human P-type ATPases as a plausible reason for the toxicity. Bacteria also expresses P-type ATPases, but genetic inactivation of all four pneumococcal P-type ATPases

Reithuber et al.
THCz: Small molecules with antimicrobial activity that block cell wall lipid intermediates

PNAS | 9 of 12
https://doi.org/10.1073/pnas.2108244118

final concentration of 5.1 μg/mL (12.5 μM) THCz-1 (1% [vol/vol] DMSO), 0.06 μg/mL penicillin (dissolved in water) and 2 μg/mL tetracycline (1% [vol/vol] DMSO) or a twofold serial dilution (*SI Appendix*, Fig. S1). The compounds were administrated in 100× stock solutions in 4-μL volumes to each well followed by thorough mixing. One percent (vol/vol) DMSO-treated cells and untreated controls were included. Sterile media samples were used to blank the measurement values. Viability determination of T4 and T4ΔlytA was performed at 30 min, 3 h, 6 h, 9 h, and 12 h following challenge by serial dilutions and spreading on blood agar plates from which colonies were counted after overnight incubation at 37 °C at 5% CO₂. Where appropriate, 100 μL of the undiluted sample was plated, providing a detection limit of 10 cfu/mL.

TEM. Pneumococcal strains T4R and T4RΔlytA (*SI Appendix*, Table S8) were prepared as for the lysis kinetic examination. Untreated cells and cells treated with 25 μM THCz-1 for 1 h were centrifuged at 6,500 × *g* for 2 min. Cell pellets were resuspended and fixed for 20 min with a 400-μL mixture of paraformaldehyde (2%) and glutaraldehyde (0.05%) in phosphate-buffered saline (PBS). Cells were then washed once with 1 mL of PBS and resuspended in 40 μL of PBS. Samples of 10 μL were placed for 2 min on carbon-coated grids (Oxford Instruments), and negative staining was performed with 2% uranyl acetate in water. Specimens were examined in a Tecnai 12 Spirit Bio TWIN TEM (FEI Company) operated at 100 kV. Digital images were recorded using a Veleta camera (Olympus Soft Imaging Solutions, GmbH).

Minimal Inhibitory Concentration Determinations. Determination of the minimal inhibitory concentration (MIC) was performed by the standardized microdilution procedure in accordance with the Performance Standards for Antimicrobial Susceptibility Testing from the Clinical and Laboratory Standards Institute (33) with the following modifications: For *S. pneumoniae* strains, the assay was done in supplemented C+Y medium and in THY medium for comparison with other bacterial species. MIC against mycobacteria were determined in cation-adjusted Mueller Hinton broth (MHB) (Oxoid) supplemented with 0.05% Tween80 (Sigma-Aldrich). *N. gonorrhoeae* was grown in tryptone soy broth (Merck) supplemented with IsoVitaleX (Becton Dickinson) according to the manufacturer's instructions. All other strains were tested using cation-adjusted MHB. Briefly, the inoculum was prepared from a liquid preculture grown to midlog phase and diluted to reach a concentration of ~5 × 10⁵ cfu/mL. Two microliters of the 100-fold concentrated serial dilutions of chemicals were added to the wells. The plates were incubated overnight at ambient atmosphere and 37 °C. For *S. aureus*, *P. aeruginosa*, and *B. subtilis* MIC determination in THY medium, the plates were incubated with shaking (~200 rpm). The MICs were determined as the lowest concentrations where no visible growth was observed. For determination of the plasma protein binding capacity of the THCz-1 compounds, bacteria were grown in C+Y medium supplemented with 10% HyClone Fetal Bovine Serum (GE Healthcare).

Cytotoxicity Assay. Lung epithelial A549 cells (ATCC CCL-185) were grown in 1× RPMI medium 1640 (Gibco) with 9% HyClone Fetal Bovine Serum (GE Healthcare) and 1× Penicillin/Streptomycin solution (Gibco). Cells were trypsinized and seeded at 1 × 10⁵ cells/mL for IC₅₀ determination (Table 2) and 1 × 10⁶ cells/mL for SAR/structure toxicity relationship (STR) investigation (*SI Appendix*, Tables S1–S3) in 100 μL of medium per well of 96-well flat bottom plates (Sarstedt) and incubated overnight at 37 °C with 5% CO₂. The antibiotic-containing medium was removed on the following day, and cells were washed with PBS. Subsequently, 100 μL of antibiotic-free medium containing the compounds in a serial dilution for IC₅₀ determination (Table 2), and concentrations of 100, 50, 25, and 12.5 μM in 1% DMSO (final concentration) for SAR/STR investigation (*SI Appendix*, Tables S1–S3) were added to the wells. After 19 h, resazurin sodium salt (Sigma) (20 μL of 440 μM in H₂O) was added to each well, and cells were further incubated for 4 h. Samples (80 μL per well) were transferred to micro test plates for immunoanalytics (Sarstedt), and absorbance was measured at 590 nm (SpectraMAX plus, Molecular Devices). Absorbance values were blanked with resazurin-containing medium, and the percentage of viable cells was calculated in comparison to solvent-treated cells. The reciprocal number for nonviable cells is given in *SI Appendix*, Tables S1–S3 for the estimation of cytotoxicity. Negative toxicity values or toxicity values of more than 100% were set to zero or 100% respectively. IC₅₀ calculation was performed using nonlinear fit log(inhibitor) vs. response calculation with variable slope and constraints with 0% and 100% toxicity for top and bottom constraints respectively in GraphPad Prism 5.04.

β-Galactosidase Reporter Assays. *B. subtilis* 168 *amyE*::pAC6 cultures with the promotor fusions P(ypuA)-*lacZ* (cell wall), P(yorB)-*lacZ* (DNA), P(yvgS)-*lacZ* (RNA), and P(yheI)-*lacZ* (protein) (34) were grown in MHB containing 5 μg/mL chloramphenicol at 30 °C to an OD(600nm) of 0.5. Subsequently, melted Mueller Hinton agar was inoculated with 1 × 10⁷ cfu/mL of the respective reporter strain. The

agar was further supplemented with 5 μg/mL chloramphenicol, and X-gal (5-Bromo-4-chloro-3-indolyl β-D-galactopyranoside) at final concentrations of 75 μg/mL (cell wall), 125 μg/mL (DNA), and 250 μg/mL (RNA and protein). After pouring and solidification of the inoculated agar, 10 μg of THCz-1, 20 μg of THCz-40, 80 μg of THCz-39, and 100 μg of THCz-5 were spotted. Three micrograms of clindamycin served as positive control for the protein reporter and as negative control for the cell wall, DNA, and RNA reporter; 6 μg of vancomycin were used as positive control for the cell wall reporter and as negative control for the protein reporter; 0.3 μg of ciprofloxacin served as positive control for the DNA reporter; and 6 μg of rifampicin were used as positive control for the RNA reporter. Results were documented after 20 h of incubation at 30 °C.

Luciferase Reporter Assays. *B. subtilis* luciferase reporter assays were conducted as previously described (35). Briefly, *B. subtilis* 168 *sacA*::pCHlux101 (P(liaI)-*lux*) was grown in MHB containing 5 μg/mL chloramphenicol at 30 °C to an OD(600nm) of 0.5. Cells were added to 96-well white wall chimney plates containing antibiotics (2 μg/mL THCz-1,128 μg/mL THCz-5, 8 μg/mL THCz-39, 4 μg/mL THCz-40, 4 μg/mL vancomycin), and luminescence measurements were performed at 30 °C in a microplate reader Spark 10M (Tecan). At least three independent biological replicate experiments were conducted.

Bacterial Cell Wall Integrity Assay. Bacterial cell wall integrity assays were adapted from previous work (36). *B. subtilis* 168 cultures were grown in MHB at 30 °C to an OD(600nm) of 0.3. Subsequently, cells were treated with 1 μg/mL THCz-1, 2 μg/mL THCz-40, 8 μg/mL THCz-39, 256 μg/mL THCz-5, 2 μg/mL vancomycin, 2 μg/mL bacitracin, 0.5 μg/mL nisin, 128 μg/mL clindamycin, 128 μg/mL ciprofloxacin, 128 μg/mL rifampicin, 128 μg/mL lysozyme, or DMSO and incubated at 30 °C. After 30 min of antibiotic exposure (treatment with lysozyme was shortened to 10 min), 200-μL culture samples were fixed in 1 mL of a 1:3 mixture of acetic acid and methanol. Five microliters of fixed cells were immobilized on a thin film of 1% wt/vol agarose containing 0.9% (wt/vol) NaCl supported on a microscope slide. Imaging was performed by phase contrast microscopy on a Zeiss Axio Observer Z1 microscope (Zeiss) equipped with an HXP 120-V light source and an Axio Cam MR3 camera. Images were acquired with ZEN 2 software (Zeiss) and analyzed and postprocessed using ImageJ v1.45s software (NIH) (37).

Antagonization Assays. Antagonization assays were performed as previously described (5). Briefly, antagonizing the antibiotic activity of THCz by potential target molecules was conducted by an MIC-type assay setup in microtiter plates. THCz-1 (5× MIC) was mixed with potential antagonists (C₅₅-P, C₅₅-PP, UDP-*N*-acetylmuramic acid pentapeptide [UDP-MurNAc-pentapeptide], lipid I, lipid II, lipid III(WTA), and lipid I(cap)) in 0.5- to 10-fold molar excess with respect to the antibiotic. *M. luteus* DSM1790 (5 × 10⁵ cfu/mL) was added, and samples were examined for visible growth after 20-h incubation. Experiments were performed in triplicate.

Quantification of Intracellular UDP-MurNAc-pp. To analyze the cytoplasmic nucleotide pool, we adapted the protocol of Kohlrausch and Höltje (38). *S. aureus* SG511 was grown in 15 mL of MHB at 37 °C to an OD(600nm) of 0.6 and incubated with 130 μg/mL chloramphenicol for 15 min. THCz-1 was added at 1×, 2.5×, and 5× MIC and incubated for another 30 min. Lipid II-complexing vancomycin (5× MIC) was used as positive control. Extraction of nucleotide-linked peptidoglycan precursors and their analysis was performed by high-pressure liquid chromatography (HPLC) as described previously (39).

Impact of THCz on Membrane-Bound Peptidoglycan Biosynthesis Reactions In Vitro. Peptidoglycan synthesis reactions were reconstituted using purified proteins and substrates in vitro. PBP2-His₆ and YbjG-His₆ were purified as described earlier (5, 39), except that PBP2 was solubilized with 0.06% Triton X-100, and additional immobilized metal ion affinity chromatography purification steps were performed.

Transglycosylation by PBP2 was determined by incubating 2 nmol of lipid II in 20 mM 2-(*N*-morpholino)ethanesulfonic acid, 2 mM MgCl₂, 2 mM CaCl₂, 0.04% Triton X-100, pH 5.5 in a total volume of 50 μL. The reaction was initiated by the addition of 8 μg of PBP2-His₆ and incubated for 2 h at 30 °C.

Dephosphorylation of C₅₅-PP was carried out using purified *S. aureus* YbjG-His₆ enzyme. Twenty nanomoles of C₅₅-PP was incubated with 1 μg of YbjG-His₆ in 20 mM Tris·HCl, 150 mM NaCl, 10 mM β-mercaptoethanol, 0.8% Triton X-100, pH 7.5 in a total volume of 50 μL for 30 min at 37 °C.

THCz were added in molar ratios ranging from 0.5 to 2 with respect to the respective substrate (C₅₅-PP or lipid II) in all in vitro assays, and samples were preincubated for 10 min prior to addition of the enzyme. Polyprenyl-containing products were extracted from the reaction mixtures with an equal volume of l-butanol/pyridine acetate, pH 4.2 (2:1, vol/vol), and analyzed by thin-layer chromatography using chloroform/methanol/water/ammonia

(88:48:10:1, vol/vol/vol/vol) as the solvent (40) and phosphomolybdic acid staining (41). Quantification was carried out using ImageJ v1.45s software (NIH) (37). Experiments were performed at least in triplicate.

Synthesis and Purification of Lipid Intermediates. Large-scale synthesis and purification of the peptidoglycan precursors lipid I and II and the wall teichoic acid precursor lipid III$_{WTA}$ was performed as previously described (5, 41). Streptococcal lipid I$_{cap}$ (undecaprenyl pyrophosphoryl glucose) was synthesized using 10 nmol of C$_{55}$-P and 100 nmol of UDP-glucose in the presence of 1.2 mg/mL 1,2-dioleoylphosphatidylglycerol, 50 mM Tris·HCl, and 10 mM MgCl$_2$. Reaction was initiated by the addition of recombinant His$_6$-CpsE, and samples were incubated for 16 h at 30°C. Lipid I$_{cap}$ was extracted from the reaction mixture and purified as described for staphylococcal capsule intermediates (42). UDP-MurNAc-pp was purified according to the protocol elaborated by Kohlrausch and Höltje (38). C$_{55}$-P and C$_{55}$-PP were purchased from Larodan Fine Chemicals AB. The concentration of purified precursors was quantified on the basis of their phosphate content as described (43).

Selection of Strains with Reduced THCz-1 Sensitivity. T4 wild-type was continuously cultured on THCz-1–containing THY agar plates which were prepared as follows: Prewarmed 2× concentrated THY medium was mixed in equal parts with autoclaved agar containing 18 g/L bacteriological agar for molecular biology (Sigma Aldrich) and 2 g/L corn starch (Maizena). Additionally, choline chloride dissolved in 2×THY was added to 10 μg/mL final concentration; 100-fold concentrated THCz-1 was mixed with 15 mL of nutrient agar in a 9-cm Petri dish and mixed thoroughly; 36 μL of freshly prepared sterile filtered catalase from bovine liver (Sigma Aldrich) dissolved to 5 mg/mL in 50 mM KPO$_4$ buffer were overlaid on the solidified agar to reach at least 24 U/mL medium. THCz-1 concentrations were increased in small incremental steps (1, 1.6, and 2 μM), and a wild-type strain was carried in parallel on chemical-free plates. Growth and lysis kinetics of pneumococci with reduced THCz-1 sensitivity originating from strain T4 (BHN1364-BHN1367) as well as knockouts (BHN1371, BHN1690, BHN1691, BHN1693, and BHN2043) in genes with point mutations (*SI Appendix*, Fig. S14)were examined in THY medium and carried out as described above, whereas THCz-1 was added in a narrow titration series of 4× MIC (3 μM, 1.2 μg/mL), 2.4× MIC (1.8 μM, 0.7 μg/mL), 2× MIC (1.5 μM, 0.6 μg/mL), and 1× MIC (0.8 μM, 0.3 μg/mL) THCz-1. T4 wild type, BHN1368, BHN1369, BHN1692, and the unencapsulated T4R were included as controls. Viability upon challenge with 2× MIC (1.5 μM, 0.6 μg/mL) THCz-1 was determined after 1 h and compared to the colony counts of the respective strain at the time of challenge for T4 wild type, T4R, and T4 *cps4E*^{G394C} (BHN1691). Pneumococcal mutant construction is described in *SI Appendix*, and used strains are described in *SI Appendix*, Table S8.

Determination of Capsular Polysaccharide Amount. *S. pneumoniae* strains were grown until midlog phase to a comparable OD and stored on ice to prevent further growth. One milliliter of the bacterial culture was lysed with 0.1% Triton X-100 (Sigma) and incubation at 37°C for 5 min and thereafter stored on ice. Protein concentration was determined with the Pierce BCA Protein Assay Kit (Thermo Scientific) according to the manufacturer's instructions, and samples were adjusted to the same protein concentration. Four microliters of a serial dilution was blotted on an Amersham Hybond-P PVDF Western blotting membrane with 0.45-μm pore size (GE Healthcare), which was activated for 30 s in ethanol and incubated 10 min thereafter in PBS, after which it was allowed to air dry briefly. Samples were allowed to dry for 1 h at 37°C, and then the membrane was blocked for 1 h with 5% BSA in PBS+0.1% Tween20 (Sigma). Pneumococcal type serum 4 (SSI Diagnostica) was incubated with T4R for 1 h at 37°C with shaking, the bacteria were pelleted thereafter, and the supernatant was spun twice for 5 min at 13,000 rpm to remove residual bacteria. The blot was incubated with the purified antibody in PBS+0.1% Tween20 overnight in 4°C. AMDEX Goat Anti Rabbit IgG Horseradish Peroxidase Conjugate (GE Healthcare) was applied for 2 h, and the blot was developed using the ECL Prime Western Blotting Detection Reagent (GE Healthcare).

Data Availability. All data are available in the main text or *SI Appendix*. Additional data for Fig. S14 are available from National Center for Biotechnology Information (PRJNA774187).

1. A. Fleming, On the antibacterial action of cultures of a penicillium, with special reference to their use in the isolation of *B. influenzae*. *Br. J. Exp. Pathol.* **10**, 226 (1929).
2. World Health Organization, *Antimicrobial Resistance: Global Report on Surveillance* (World Health Organization, 2014).
3. H. Kresse, M. J. Belsey, H. Rovini, The antibacterial drugs market. *Nat. Rev. Drug Discov.* **6**, 19–20 (2007).
4. K. Bush, P. A. Bradford, β-Lactams and β-lactamase inhibitors: An overview. *Cold Spring Harb. Perspect. Med.* **6**, a025247 (2016).
5. L. L. Ling *et al.*, A new antibiotic kills pathogens without detectable resistance. *Nature* **517**, 455–459 (2015).
6. A. Müller, A. Klöckner, T. Schneider, Targeting a cell wall biosynthesis hot spot. *Nat. Prod. Rep.* **34**, 909–932 (2017).
7. A. J. F. Egan, J. Errington, W. Vollmer, Regulation of peptidoglycan synthesis and remodelling. *Nat. Rev. Microbiol.* **18**, 446–460 (2020).
8. I. G. Boneca, G. Chiosis, Vancomycin resistance: Occurrence, mechanisms and strategies to combat it. *Expert Opin. Ther. Targets* **7**, 311–328 (2003).
9. F. Grein, T. Schneider, H. G. Sahl, Docking on lipid II-A widespread mechanism for potent bactericidal activities of antibiotic peptides. *J. Mol. Biol.* **431**, 3520–3530 (2019).
10. J. Medeiros-Silva, S. Jekhmane, E. Breukink, M. Weingarth, Towards the native binding modes of antibiotics that target lipid II. *ChemBioChem* **20**, 1731–1738 (2019).
11. F. Grein *et al.*, Ca²⁺-Daptomycin targets cell wall biosynthesis by forming a tripartite complex with undecaprenyl-coupled intermediates and membrane lipids. *Nat. Commun.* **11**, 1455 (2020).
12. A. Tomasz, S. Waks, Mechanism of action of penicillin: Triggering of the pneumococcal autolytic enzyme by inhibitors of cell wall synthesis. *Proc. Natl. Acad. Sci. U.S.A.* **72**, 4162–4166 (1975).
13. L. Su *et al.*, Design, synthesis and evaluation of hybrid of tetrahydrocarbazole with 2,4-diaminopyrimidine scaffold as antibacterial agents. *Eur. J. Med. Chem.* **162**, 203–211 (2019).
14. P. Mellroth *et al.*, LytA, major autolysin of *Streptococcus pneumoniae*, requires access to nascent peptidoglycan. *J. Biol. Chem.* **287**, 11018–11029 (2012).
15. A. Typas, M. Banzhaf, C. A. Gross, W. Vollmer, From the regulation of peptidoglycan synthesis to bacterial growth and morphology. *Nat. Rev. Microbiol.* **10**, 123–136 (2011).
16. A. Urban *et al.*, Novel whole-cell antibiotic biosensors for compound discovery. *Appl. Environ. Microbiol.* **73**, 6436–6443 (2007).
17. D. A. Wirtz *et al.*, Biosynthesis and mechanism of action of the cell wall targeting antibiotic hypeptin. *Angew. Chem. Int. Ed. Engl.* **60**, 13579–13586 (2021).
18. T. Mascher, S. L. Zimmer, T. A. Smith, J. D. Helmann, Antibiotic-inducible promoter regulated by the cell envelope stress-sensing two-component system LiaRS of *Bacillus subtilis*. *Antimicrob. Agents Chemother.* **48**, 2888–2896 (2004).
19. H. Strahl, L. W. Hamoen, Membrane potential is important for bacterial cell division. *Proc. Natl. Acad. Sci. U.S.A.* **107**, 12281–12286 (2010).
20. M. Bublitz *et al.*, Tetrahydrocarbazoles are a novel class of potent P-type ATPase inhibitors with antifungal activity. *PLoS One* **13**, e0188620 (2018).
21. R. T. Cartee, W. T. Forsee, M. H. Bender, K. D. Ambrose, J. Yother, CpsE from type 2 *Streptococcus pneumoniae* catalyzes the reversible addition of glucose-1-phosphate to a polyprenyl phosphate acceptor, initiating type 2 capsule repeat unit formation. *J. Bacteriol.* **187**, 7425–7433 (2005).
22. J. C. Paton, C. Trappetti, *Streptococcus pneumoniae* capsular polysaccharide. *Microbiol. Spectr.*, 10.1128/microbiolspec.GPP3-0019-2018 (2019).
23. J. Flores-Kim, G. S. Dobihal, A. Fenton, D. Z. Rudner, T. G. Bernhardt, A switch in surface polymer biogenesis triggers growth-phase-dependent and antibiotic-induced bacteriolysis. *eLife* **8**, e44912 (2019).
24. T. Homma *et al.*, Dual targeting of cell wall precursors by teixobactin leads to cell lysis. *Antimicrob. Agents Chemother.* **60**, 6510–6517 (2016).
25. P. Mellroth *et al.*, Structural and functional insights into peptidoglycan access for the lytic amidase LytA of *Streptococcus pneumoniae*. *MBio* **5**, e01120–e13 (2014).
26. T. Sandalova *et al.*, The crystal structure of the major pneumococcal autolysin LytA in complex with a large peptidoglycan fragment reveals the pivotal role of glycans for lytic activity. *Mol. Microbiol.* **101**, 954–967 (2016).
27. M. Schlag *et al.*, Role of staphylococcal wall teichoic acid in targeting the major autolysin Atl. *Mol. Microbiol.* **75**, 864–873 (2010).
28. T. V. Akalaeva *et al.*, Antitubercular, antifungal, and antibacterial activity in vitro of 1-phenethylamino-1,2,3,4-tetrahydrocarbazoles. *Pharm. Chem. J.* **24**, 826–829 (1990).
29. A. J. Hutt, J. O'Grady, Drug chirality: A consideration of the significance of the stereochemistry of antimicrobial agents. *J. Antimicrob. Chemother.* **37**, 7–32 (1996).

Reithuber et al.
THCz: Small molecules with antimicrobial activity that block cell wall lipid intermediates

PNAS | 11 of 12
https://doi.org/10.1073/pnas.2108244118

MICROBIOLOGY

30. P. Edebrink *et al.*, Structural studies of the O-polysaccharide from the lipopolysaccharide of *Moraxella (Branhamella) catarrhalis* serotype A (strain ATCC 25238). *Carbohydr. Res.* **257**, 269–284 (1994).

31. T. Schneider *et al.*, Plectasin, a fungal defensin, targets the bacterial cell wall precursor Lipid II. *Science* **328**, 1168–1172 (2010).

32. C. Brunati *et al.*, Expanding the potential of NAI-107 for treating serious ESKAPE pathogens: Synergistic combinations against Gram-negatives and bactericidal activity against non-dividing cells. *J. Antimicrob. Chemother.* **73**, 414–424 (2018).

33. Clinical Laboratory Standards Institute, *Methods for Dilution Antimicrobial Susceptibility Tests for Bacteria That Grow Aerobically; Approved Standard* (Clinical and Laboratory Standards Institute, Wayne, PA, ed. 9, 2012).

34. H. Harms *et al.*, Antimicrobial dialkylresorcins from marine-derived microorganisms: Insights into their mode of action and putative ecological relevance. *Planta Med.* **84**, 1363–1371 (2018).

35. S. Tan, K. C. Ludwig, A. Müller, T. Schneider, J. R. Nodwell, The lasso peptide siamycin-I targets lipid II at the Gram-positive cell surface. *ACS Chem. Biol.* **14**, 966–974 (2019).

36. M. Wenzel *et al.*, Proteomic response of *Bacillus subtilis* to lantibiotics reflects differences in interaction with the cytoplasmic membrane. *Antimicrob. Agents Chemother.* **56**, 5749–5757 (2012).

37. C. A. Schneider, W. S. Rasband, K. W. Eliceiri, NIH Image to ImageJ: 25 years of image analysis. *Nat. Methods* **9**, 671–675 (2012).

38. U. Kohlrausch, J. V. Höltje, Analysis of murein and murein precursors during antibiotic-induced lysis of *Escherichia coli*. *J. Bacteriol.* **173**, 3425–3431 (1991).

39. T. Schneider *et al.*, The lipopeptide antibiotic Friulimicin B inhibits cell wall biosynthesis through complex formation with bactoprenol phosphate. *Antimicrob. Agents Chemother.* **53**, 1610–1618 (2009).

40. P. D. Rick *et al.*, Characterization of the lipid-carrier involved in the synthesis of enterobacterial common antigen (ECA) and identification of a novel phosphoglyceride in a mutant of *Salmonella typhimurium* defective in ECA synthesis. *Glycobiology* **8**, 557–567 (1998).

41. T. Schneider *et al.*, In vitro assembly of a complete, pentaglycine interpeptide bridge containing cell wall precursor (lipid II-Gly5) of *Staphylococcus aureus*. *Mol. Microbiol.* **53**, 675–685 (2004).

42. M. Rausch *et al.*, Coordination of capsule assembly and cell wall biosynthesis in *Staphylococcus aureus*. *Nat. Commun.* **10**, 1404 (2019).

43. G. Rouser, S. Fkeischer, A. Yamamoto, Two dimensional then layer chromatographic separation of polar lipids and determination of phospholipids by phosphorus analysis of spots. *Lipids* **5**, 494–496 (1970).

44. P. García, M. P. González, E. García, R. López, J. L. García, LytB, a novel pneumococcal murein hydrolase essential for cell separation. *Mol. Microbiol.* **31**, 1275–1281 (1999).

45. R. G. Kansal, A. McGeer, D. E. Low, A. Norrby-Teglund, M. Kotb, Inverse relation between disease severity and expression of the streptococcal cysteine protease, SpeB, among clonal M1T1 isolates recovered from invasive group A streptococcal infection cases. *Infect. Immun.* **68**, 6362–6369 (2000).